16[th] World Conference on Earthquake, 16WCEE 2017
Santiago Chile, January 9th to 13th 2017
Paper N° 2341
Registration Code: S-E1463069267

INTEGRATED ANALYSIS OF REINFORCED CONCRETE COLUMNS RETROFITTED WITH FIBRE-REINFORCED POLYMER

V. Sadeghian[(1)], O. Kwon[(2)] and F. Vecchio[(3)]

[1]PhD candidate, Dept. of Civil Engineering, Univ. of Toronto, 35 St. George St., Toronto, ON, Canada, M5S 1A4, (corresponding author). E-mail: Vahid.sadeghian@utoronto.ca
[2]Associate professor, Dept. of Civil Engineering, Univ. of Toronto, 35 St. George St., Toronto, ON, Canada, M5S 1A4. E-mail: os.kwon@utoronto.ca
[3]Professor, Dept. of Civil Engineering, Univ. of Toronto, 35 St. George St., Toronto, ON, Canada, M5S 1A4. E-mail: fjv@ecf.utoronto.ca

Abstract

Use of fibre-reinforced polymer (FRP) in the strengthening of seismic-deficient columns is becoming increasingly common; however, the nonlinear analysis of frame structures containing such members poses several challenges. At the component-level, analyzing damage effects, confinement enhancement, buckling of longitudinal bars, and bond-slip effects at the interface of concrete and FRP sheets require finely detailed finite element (FE) models. At the system-level, force redistribution due to stiffness changes between different components can affect the response of the column, especially when the structure experienced damage prior to retrofitting. An integrated framework was recently developed which enables analysis of reinforced concrete (RC) structures at both the component- and system-level in a concurrent fashion. In this modelling approach, the critical components of the structure such as retrofitted columns are modelled in a detailed FE program while the rest of the structure is modelled in a computationally efficient frame analysis program. Herein, the application of the framework to retrofitted columns is demonstrated by modelling and analyzing several test specimens. The procedure is found to simulate the experimental behaviour of the specimens examined with a high level of accuracy. The influence of damage effects, FRP-related mechanisms, and buckling of longitudinal bars are investigated in detail. In addition, the strength and ductility enhancement effects of RC columns repaired with FRP wraps are demonstrated at system-level through multi-scale modelling of a bridge structure.

Keywords: Reinforced concrete; Fibre reinforced polymer; Nonlinear analysis; Multi-scale simulation; Substructuring technique.

1. Introduction

In recent years, many studies have shown the effectiveness of fibre-reinforced polymer (FRP) composites in improving the ductility and hence the energy dissipation capacity of damaged or seismically deficient reinforced concrete (RC) columns. Based on the experimental studies, different uniaxial stress-strain relationships have been proposed for confinement enhancement of concrete due to FRP wraps. Lam and Teng [1] provided an extensive review of the previous test results and compared them with the available models. They demonstrated that there is a large scatter in terms of level of effectiveness of FRP confinement which was associated with inaccuracy in reported FRP material properties. They also concluded that while some complicated models [2, 3] can predict the confinement behaviour with a high level of accuracy, the relationship between the strength of confined concrete and FRP lateral confining pressure can be closely approximated with a simple linear formula.

Although uniaxial compression models have enabled researchers to compute the response of plain concrete confined with FRP at the material-level, they do not fully represent the behaviour of retrofitted RC columns at the structural-level which is influenced by the interaction between cracked concrete, reinforcing bars, and FRP wraps under combined axial, shear, and bending forces. Some experimental studies have investigated the structural-level response of repaired RC columns under general loading conditions [4]. However, there is limited research on composite modelling and analysis approaches. Zhu et al. [5] modelled concrete-filled FRP tube columns in OpenSees software [6] using nonlinear fibre beam elements. The confinement model of Samaan et al. [7] was incorporated into a simplified concrete hysteresis model by Taucer et al. [8] which could not consider cyclic damage of concrete. Teng et al. [9] used a similar modelling approach while considering cyclic stress deterioration of concrete using the Lam and Teng model [10]. Both studies had limitations such as assuming plane sections normal to the element axis remain plane during bending and neglecting bond-slip effects between FRP and concrete. Rougier and Luccioni [11] analyzed circular RC columns confined with carbon-fiber-reinforced polymer (CFRP) under concentric axial loads. The behaviour of concrete under triaxial compression was captured using a modified plastic damage model. The model was derived based on a calibration process and required a large number of input parameters. In addition, the analysis was performed in a monotonic loading manner and the accuracy of the model in capturing cyclic damage effects was not verified.

Some experimental studies have reported bar buckling as a critical mechanism in the response of retrofitted RC columns [4]. However, most analysis procedures including the abovementioned studies neglected this effect. Karabinis et al. [12] performed a numerical study on the effectiveness of CFRP confinement in preventing buckling of longitudinal bars in concrete columns subjected to concentric axial loads using ABAQUS software [13]. A modified Drucker-Prager type model was used to represent the triaxial compression behaviour of concrete and define the failure criterion. The model required estimation of a friction value and a plastic dilatation parameter for concrete. The buckling behaviour of steel bars was taken into account according to the Yalcin and Saatcioglou model [14]. Although the analysis procedure was able to accurately capture the monotonic response of heavily confined RC columns (i.e. four layers of FRP), it significantly underestimated the ductility of columns with lower levels of confinement (i.e. one layer of FRP) due to premature buckling failure of steel bars.

Furthermore, the majority of numerical studies have considered crushing of concrete and rupture of steel bars or FRP as possible failure modes and have neglected the shear behaviour. Montoya et al. [15] implemented a confined concrete model into VecTor3 software which is capable of considering shear behaviour in detail. However, the study was limited to monotonic concentric axial loading condition and did not consider slippage of FRP or buckling of steel bars.

Most importantly, almost all previous studies have been performed at the component-level. There are a few studies which attempted to model the entire structural system while considering the RC components confined with FRP. However, they neglected shear behaviour and oversimplified FRP-related mechanisms [16], or required the user to input force-displacement relationship for each member [17], or introduced a calibrated stiffness degradation factor to capture damage accumulation [18] which raises questions about the applicability of the method to other structural systems.

In summary, available numerical procedures have been shown to be capable of capturing the response of RC columns strengthened with FRP under monotonic concentric axial loads. However, they have limitations in considering one or more of the following four factors: 1) General loading condition: combined axial, shear, and bending forces in a cyclic or reversed cyclic manner; 2) FRP-related mechanics: slippage between FRP and concrete and tension stiffening effects; 3) RC-related mechanisms: damage effects prior to repair and buckling of reinforcing bars; 4) Influence of component-level behaviour on the system-level response and vice versa. This study demonstrates the application of a recently developed integrated framework, Cyrus, in analyzing RC columns retrofitted (i.e. initially undamaged) or repaired (i.e. initially damaged) with FRP sheets under a general loading condition. The integrated framework performs the analysis at both the component-level and system-level in a concurrent manner. The analysis procedure is based on the Disturbed Stress Field Model [19] which have been shown to be capable of capturing the shear behaviour of cracked RC. At the component-level analysis, appropriate constitutive relationships are adopted to accurately model each material module and address the above-mentioned deficiencies in terms of their interactions. Application examples at both the component-level and system-level will be provided.

2. Analysis Framework

The proposed multi-scale analysis procedure consists of three main components: an integration module, substructure modules, and interface modules. A brief description of each part along with references for further information are provided in the following sections.

2.1 Integration module

Typically, modelling an entire structural system in a detailed FE program is not practical due to the complicated analysis procedure and high computational demand. On the other hand, system-level analysis tools are not able to capture detailed behaviour of RC members confined with FRP. An integration module, named Cyrus, was recently developed by the authors [20] which can combine different analysis tools while fully taking into account the interaction between the substructures. The repaired members along with other critical components of the structure can be modelled in a detailed FE program while the rest of the structure is modelled in another program using fibre beam elements. The coupled formulation of the analysis enables the consideration of force redistribution due to stiffness changes between different components. Moreover, the integration module enables the use of the parallel processing technique to avoid computational time and memory storage limitations associated with sequential single-platform analyses.

2.2 Substructure modules

In this study, FRP-confined RC columns were modelled and analyzed using the VecTor2 program, a two-dimensional nonlinear FE software for RC structures. The program uses a smeared, rotating crack formulation according to the Disturbed Stress Field Model (DSFM) [19]. The DSFM has been shown to be capable of accurately representing the behaviour of cracked RC members particularly under shear. In terms of analyzing the RC components with FRP wraps, appropriate models were used to take into account concrete confinement enhancement, tension stiffening effects, bond-slip effects at the interface, and buckling of reinforcing bars. In addition, damage effects and spalling of concrete cover prior to repair of columns were considered. A brief description of modelling procedure for aforementioned mechanical effects is presented in the subsequent sections.

While the critical components were modelled in a detailed FE program, the rest of the structure was modelled in a frame analysis program using lower-dimensional elements. Cyrus is compatible with two different analysis programs which provide computational and memory efficient frame type elements: VecTor5 [21] and OpenSees [6]. OpenSees provides elastic beam-column elements which have rotational springs at the ends to represent the nonlinear behaviour, suitable for flexure-critical structures. VecTor5 is a nonlinear fibre analysis program based on the unbalanced force approach which can consider shear-related effects. In this study, to account for shear mechanisms, VecTor5 was chosen for modelling the non-critical members.

2.3 Interface modules

One of the main challenges in a multi-scale simulation is the modelling of mixed-dimensional interfaces between the sub-models. Recently, a new interface element, named the F2M element, was developed by the authors for membrane-beam mixed-dimensional connection. The F2M element is a two-node semi-deformable element that can fully transfer translational and rotational displacements at the interface. The stiffness matrix of the element was formulated such that it has high stiffness values in the transverse and rotational directions while zero stiffness in the axial direction. It computes the stress distribution at the interface of frame sub-model based on DSFM model, and applies the equivalent forces in the opposite direction on the connecting membrane elements. Compared to the traditional rigid interface method, the F2M interface element does not add any additional stiffness to the system and allows lateral expansion. Compared to other common types of interface methods such as the multi-point-constraints approach and transition elements, the proposed method takes into account the nonlinear behaviour of the structure at the interface and provides a much more accurate shear stress distribution at the connection section.

A detailed description of the integration module and F2M interface element are provided in the Cyrus User's Manual [22]. Fig.1 demonstrates application of the proposed multi-scale modelling procedure on a bridge structure with repaired RC columns.

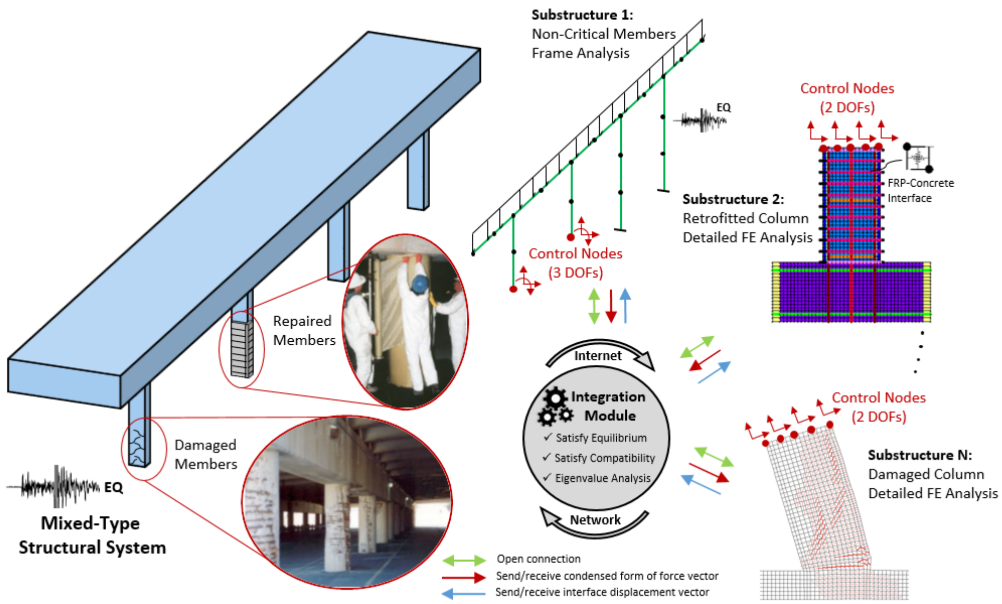

Fig. 1 - Overview of the proposed multi-scale analysis approach

3. Modelling RC-Related Mechanisms

In this section, mechanisms which have not been fully considered in the previous studies will be described briefly. For more information on material constitutive models and second-order material effects, refer to the description of default models in the VecTor2 User's Manual [23].

The hysteresis response of concrete and steel bars were modelled according to the Vecchio [24] and Seckin [25] models, respectively. In the analysis procedure, total concrete and reinforcement strains were formulated to take into account plastic offset strains caused by concrete damage and yielding of reinforcement under cyclic loads. To track the plastic offset strains and compute maximum and minimum strains obtained during previous cycles, a set of transformation equations based on the Mohr's circle approach were used. This enabled the analysis to define the strain values in any arbitrary direction (local x and y, or principal 1 and 2) and be consistent with rotating crack formulations, meaning the principal strain directions are free to rotate.

RC columns under cyclic loads can experience a softening behaviour before reaching the ultimate stress value defined in their constitutive relationships. This behaviour initiates due to spalling of concrete cover and extends as buckling of longitudinal reinforcements occur. A cover spalling criterion was introduced in which the principal net compressive strain, crack width, and crack inclination were limited to -3.5×10^{-3} mm/mm, 2.0 mm, and 30.0 degrees, respectively. According to this criterion, if an element located in the concrete cover zone reaches one of these limits, the element will be deactivated, meaning that its strength and stiffness will be set to near-zero values. In addition to providing more realistic analysis results, considering the cover spalling mechanism significantly improves the stability of unloading and reloading portions of the load-deflection response, particularly under high deformations.

The buckling of the longitudinal bars were considered using the Dhakal and Maekawa model [26]. The model assumes linear reduction of steel compressive stress from yielding point (f_y, ε_y) to an intermediate point (f_i, ε_i). After the intermediate point, a constant negative stiffness of $0.02E_s$ is assumed until compressive stress reaches $0.2f_y$. The intermediate point is determined based on Eq. (1) to Eq. (4).

$$r_b = \sqrt{\frac{f_y}{100}}\frac{L}{D} \tag{1}$$

$$\varepsilon_i = \varepsilon_y[55 - 2.3r_b] \geq 7\varepsilon_y \tag{2}$$

$$f_i = f_{it}\alpha(1.1 - 0.016r_b) \geq 0.2f_y \tag{3}$$

$$0.75 \leq \alpha = 0.75 + \frac{\varepsilon_u - \varepsilon_{sh}}{300\varepsilon_y} \leq \min(\frac{f_u}{1.5f_y}, 1.0) \tag{4}$$

where r_b is the slenderness ratio and f_{it} is the stress in the original curve corresponding to the intermediate strain ε_i. The graphical demonstration of the model is provided in Fig.2.

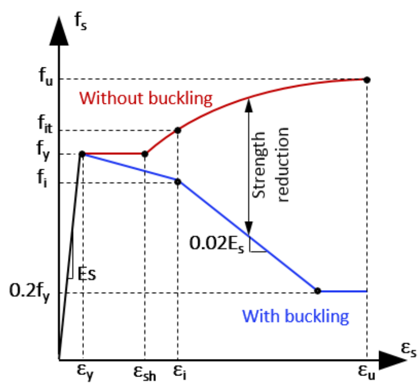

Fig. 2 - Graphical demonstration of Dhakal and Makeawa reinforcement buckling model [26]

To simulate the damage effects prior to repair of RC columns, the analysis was performed in two separate stages. In the first stage, which represented the column prior to the repair, the elements and materials related to the FPR wraps were deactivated in the model. Similar to the experimental procedure, the analysis was performed until the concrete cover started to spall off. In the second stage, which represented the column after repair, the FRP elements and materials were activated in the model. Using a binary file which stores the strain and stress history of the structure, the damage effects prior to repair was taken into account and the analysis was resumed and continued until failure.

4. Modelling FRP-Related Mechanisms

In the detailed FE sub-model, two-node truss elements were used to model FRP sheets. A uniform cross-sectional area computed from the thickness and tributary width of the FRP sheets was assigned to the truss elements. The stress-strain response was assumed linear-elastic up to the rupture of FRP in tension and zero stress in compression.

To model bond-slip effects accurately, link elements were used at the interface of RC elements and FRP truss elements. The bond stress-strain relationship was computed based on the Nakaba et al. model [27]. This bilinear bond model is based on concrete fracture energy and expressed by Eq. (5) to Eq. (8).

$$\tau_{bFy} = (54f_c')^{0.19} \tag{5}$$

$$S_{Fy} = 0.057 G_F^{0.5} \tag{6}$$

$$G_F = \left(\frac{\tau_{bFy}}{6.6}\right)^2 \tag{7}$$

$$S_{Fu} = \frac{2G_F}{\tau_{bFy}} \tag{8}$$

where τ_{bFy}, f'_c, S_{Fy}, G_F, and S_{Fu} are the maximum bond shear stress, compressive strength of concrete, bond slip at the maximum shear stress, fracture energy of concrete, and ultimate bond slip, respectively. For specimens which experienced separation of FRP sheets from concrete at the failure, as recommended by Wong and Vecchio [28], the maximum bond stress was reduced to the modulus of rupture of concrete (f_r).

$$f_r = 0.6 \times (f'_c)^{0.5} \tag{9}$$

Crack formation is another factor which can influence the behaviour of retrofitted RC members. FRP sheets can control crack width and reduce crack spacing. Also, premature debonding of the sheets, before reaching the desired strength, can initiate from crack locations and is greatly influenced by crack spacing. In this study, the crack formation and tension stiffening effects were considered using the Sato and Vecchio model [29]. The model computes crack spacing and contribution of FRP to tensile strength by formulating the equilibrium at the crack location based on the Tension Chord concept.

In addition, the confinement effects of FRP wraps were simulated with a smeared out-of-plane FRP component in the concrete element. The out-of-plane stresses and strains were utilized to compute the strength and ductility enhancements due to the confinement. The out-of-plane concrete strain was computed by Eq. (10).

$$\varepsilon_{cz} = \frac{-E_c}{E_c + \rho_{Fz} E_F}\left(\nu_{12}\frac{f_{c2}}{\overline{E}_{c2}} + \nu_{21}\frac{f_{c1}}{\overline{E}_{c1}}\right) \tag{10}$$

where E_c, $\overline{E}_c$, f_c, ν are the initial stiffness, secant stiffness, stress, and Poisson's ratio of concrete; E_F is the stiffness of FRP; and ρ_{Fz} is the FRP ratio in the Z-direction which is equal to the cross-sectional area of out-of-plane FRP sheets divided by the area of concrete. Subscripts 1 and 2 indicate in-plane principal stress directions.

Satisfying equilibrium, the out-of-plane concrete compressive stress, f_{cz}, was determined from Eq. (11).

$$f_{cz} = -\rho_{Fz} \times f_{Fz} \tag{11}$$

where f_{Fz} is the stress in the out-of-plane FRP sheet which was calculated based on Eq. (12) and must be less than the ultimate strength of FRP (f_{FU}).

$$f_{Fz} = E_F \varepsilon_{cz} \leq f_{FU} \tag{12}$$

A more detailed description of modelling procedures for FRP-related mechanics are provided in [30].

5. Application Examples

5.1 Component-level example: seismically deficient RC columns

Memon and Sheikh [4] examined the seismic resistance of large-scale square RC columns with insufficient confinement constructed according to the pre-1971 design codes. The test program consisted of five columns retrofitted with GFRP wraps, two columns damaged and then repaired with GFRP wraps, and a control column to assess the benefits of retrofitting. Specimens were tested under constant axial load and cyclic lateral load simulating seismic loading conditions. The test parameters were the number of

GFRP layers, the axial load, and the presence of column damage (Table 1). The specimen represented a portion of a column in a bridge or building between the section of maximum moment and the point of contraflexure.

Table 1 - Details of the RC column test specimens

Specimen	**GFRP Wrap**	**Axial Load (P/Po)**	**Description**	**Damaged Zone (mm) Test**	**Analysis**
AS-1NSS	None	0.56	Control	458	400
ASG-2NSS	2 Layers	0.33	Retrofitted	188	180
ASG-3NSS	4 Layers	0.56	Retrofitted	207	200
ASG-4NSS	2 Layers	0.56	Retrofitted	189	180
ASG-5NSS	1 Layers	0.33	Retrofitted	202	180
ASG-6NSS	6 Layers	0.56	Retrofitted	204	180
ASGR-7NSS	2 Layers	0.33	Repaired	179	160
ASGR-8NSS	6 Layers	0.56	Repaired	199	200

As shown in Fig.3, the multi-scale model consisted of two components: a detailed FE sub-model which had the capability to analyze repaired structures, and a computationally fast frame sub-model. The two-dimensional detailed FE sub-model was created using 8-DOF RC rectangular elements with 20mm × 20mm mesh size. All the reinforcement was modelled as discrete using 4-DOF steel truss elements, except the transverse reinforcement of the stub which was modelled as smeared. The loading plate was modelled using structural steel rectangular elements. The GFRP sheets were modelled with discrete truss bars which were indirectly attached to the underlying RC rectangular elements via link elements. Due to the high axial force of the columns, instead of applying the confinement enhancements to boundary elements, it was distributed through the height of the section to avoid premature failure of core elements. Since the GFRP was applied as a wrap, it was assumed that there is no slip at the corner nodes. This was modelled by using perfect bond between GFRP and concrete for boundary nodes at the top and bottom sections.

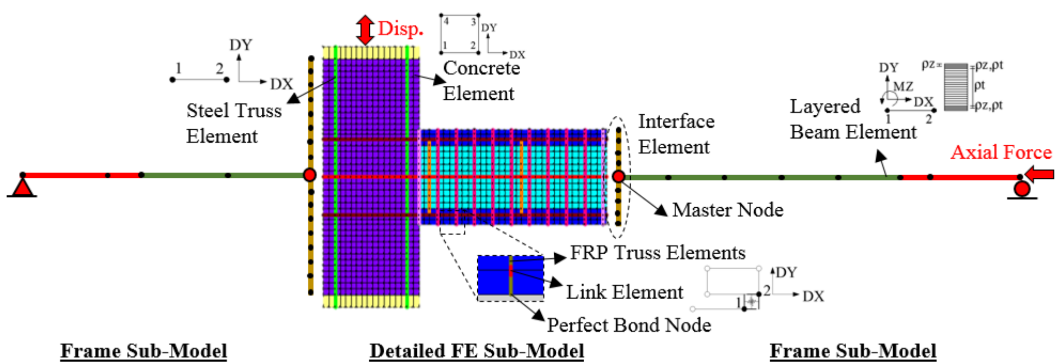

Fig. 3 - Mixed-type FE model for RC column

The analytical and experimental peak loads in positive and negative cycles are compared in Table 2. As an example, the load-deflection responses of two specimens (AS-1NSS and ASG-6NSS) are presented in Fig.4. In general, the computed responses agreed reasonably well with the experimentally observed behaviour. The multi-scale analysis was able to accurately capture the strength degradation under repeated cycles at the same applied displacement. Also, the computed pinching effects correlated well with the experimental results. For specimens with more than two layers of GFRP, the analysis had a tendency to overestimate the peak load. This might be because of the possible slip between GFRP layers or lower confinement enhancement due to arching effect in square columns. Neither of these mechanism were considered in the analysis.

Table 2 – Experimental and numerical peak loads for RC column specimens

Specimen	Experimental Peak Load (kN)			Numerical Peak Load (kN)			Num/Exp
	Positive	**Negative**	**Average**	**Positive**	**Negative**	**Average**	
AS-1NSS	327	-293	310	324	-305	314	1.01
ASG-2NSS	371	-317	344	392	-359	375	1.09
ASG-3NSS	364	-318	341	397	-371	384	1.13
ASG-4NSS	342	-269	306	378	-319	349	1.14
ASG-5NSS	375	-334	354	392	-372	382	1.08
ASG-6NSS	419	-370	395	447	-424	435	1.10
ASGR-7NSS	363	-310	337	382	-369	376	1.11
ASGR-8NSS	355	-362	358	391	-355	373	1.04
						Mean	1.09
						COV (%)	3.9

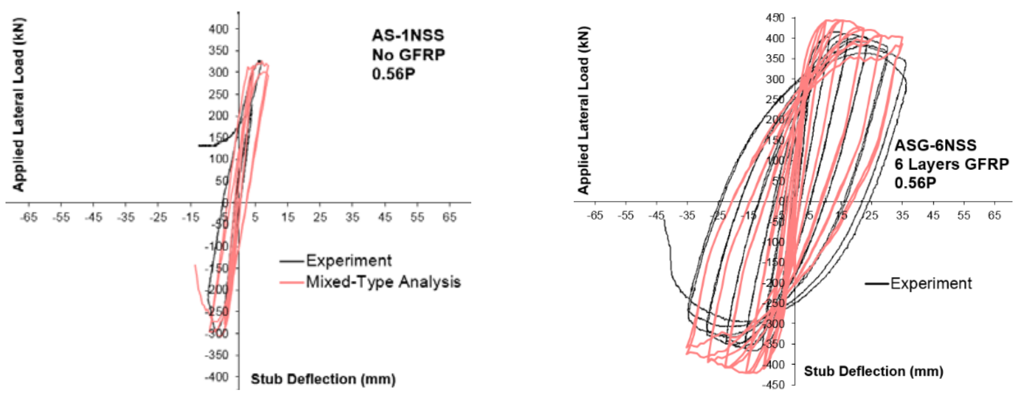

Fig. 4 - Analytical and experimental load-deflection responses for AS-1NSS and ASG-6NSS specimens

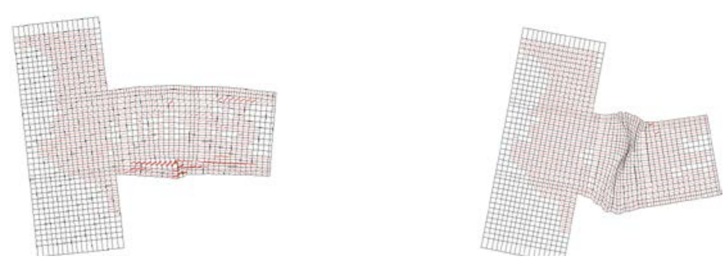

(a) (b)

Fig. 5 - Computed failure mode: (a) column without GFRP; (b) column with two layers of GFRP

In terms of the failure mode, the control column showed a different behaviour compared to the other columns which were strengthened with GFRP (Fig.5). In the control specimen, the failure was initiated by spalling of the concrete followed by yielding of the transverse reinforcement and buckling of the longitudinal bars. On the other hand, in the retrofitted specimens, no concrete spalling was observed due the high confinement provided by GFRP wraps. In these specimens, the failure occurred due to rupture of GFRP sheets. The mixed-type analysis predicted similar damage sequences and failure modes.

All the specimens experienced buckling of longitudinal reinforcement prior to failure. As shown in Fig.6 (a), without considering the buckling behaviour the analysis significantly overestimates the peak load and post-peak strength.

For the two repaired specimens (ASG-7NSS-R and ASG-8NSS-R) which were initially damaged and then strengthened with GFRP, the analysis response was greatly affected by the level of axial load. Under low level of axial force ($0.33P_o$), the comparison of the computed response of initially damaged specimen (ASG-7NSS-R) with the similar undamaged specimen (ASG-2NSS), indicated that the damage only affected the initial cycles and the overall behaviour of the specimens were similar. However, under higher level of axial force ($0.56P_o$), the damage effects were much more pronounced. In this case, the initially damaged specimen (ASG-8NSS-R) showed significantly lower strength and ductility compared to the similar undamaged specimen (ASG-6NSS). A similar behaviour was observed in the experiment. Fig.6 (b) shows the influence of damage effects on the response of the column under high axial force for both experiment and analysis.

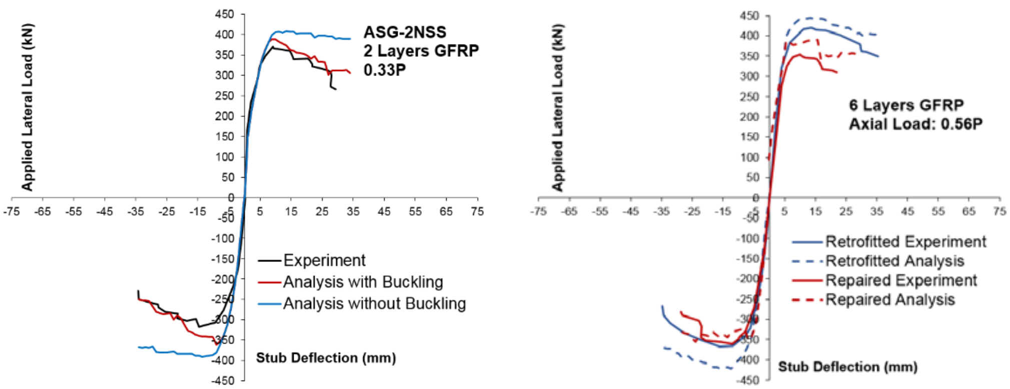

(a) (b)

Fig. 6 - Influence of: (a) bar buckling and (b) damage effects on the behaviour of RC columns

5.2 System-level example: RC bridge with critical piers

The behaviour of a RC bridge structure strengthened with FRP wraps was investigated at both the system-level and the component-level. The bridge had four 10m long spans supported by three piers with the height of 3m. The connections between the deck and piers were assumed to be pinned connections. The cross sections of the piers were identical to the cross section of the RC columns described in the previous application example. The level of axial force in Pier 1, Pier 2, and Pier 3 was selected as $0.56P_o$, $0.33P_o$, and $0.10P_o$, respectively. It must be noted that this is an illustration example and the structural details and loading configuration do not represent a real structure.

First, a stand-alone frame analysis was conducted which indicated formation of plastic hinges at the base of the piers. For a more detailed analysis of the structure, the lower portions of the piers were modelled in VecTor2 while the rest of the structure was modelled in a frame analysis software (Fig.7). The multi-scale analysis revealed more details about the response of the system and the critical components. The failure initiated by spalling of concrete cover at about 300 mm from the base of Pier 1 which was followed by buckling of the longitudinal bars and crushing of the concrete core. The force redistribution between the three piers under monotonically increasing lateral displacement is demonstrated in Fig.8 (a). Zone 1 corresponds to extensive cracking of Pier 3 on the tension side, which resulted in a reduction in its force capacity and consequently a large increase in the percentages of force carried by Pier 1 and Pier 2. Zone 2 indicates a significant force redistribution from Pier 1 to Pier 2 and Pier 3 due to spalling of the concrete cover, buckling of the longitudinal bars, and crushing of some of the concrete core elements. Zone 3 and Zone 4 correspond to tensile yielding of the longitudinal bars in Pier 3 and extensive crushing of the concrete core elements in Pier 1, respectively. A comparison of the graphs in all four zones (Fig.8) clearly shows that as the force capacity percentage in Pier 1 reduces due to failure mechanisms, Pier 2 and Pier 3 must carry higher percentages of the total lateral force.

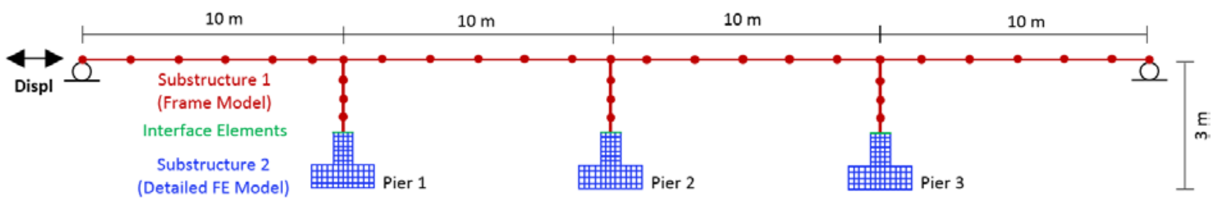

Fig. 7 – Multi-Scale FE model of a RC bridge with critical piers

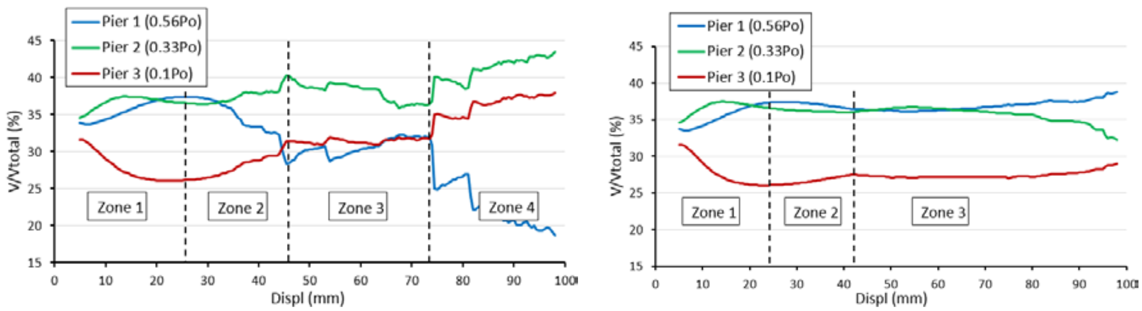

(a) (b)

Fig. 8 – Force redistribution in RC bridge piers: (a) without GFRP; (b) Pier 1 confined with GFRP

In the next phase of the analysis, the base of the most critical pier, Pier 1, was confined with 6 layers of GFRP using a similar modelling procedure as described in the previous application example. The analysis results showed a significant increase in strength and ductility of the structure (Fig.9). In addition, there was a much more stable force distribution between the three piers compared to the prior to repair analysis case. As a result of GFRP confinement, the buckling of longitudinal bars in Pier 1 was prevented. Failure occurred by crushing of the concrete core elements in Pier 1 and Pier 2 (Zone 2) and shortly after in Pier 3 (Zone 3).

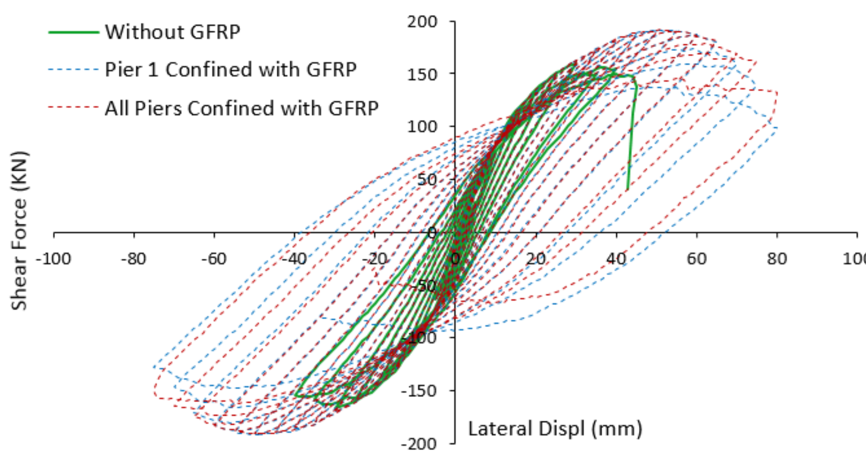

Fig. 9 – Load-deflection response of RC bridge prior and after repair with GFRP

In the last phase of the analysis, the base of the remaining piers (Pier 2 and Pier 3) were confined. However, the analysis results indicated an almost identical load-deflection response as the previous analysis case. The reason is that when Pier 1 loses its strength due to crushing of its concrete core elements, it imposes additional force on Piers 2 and 3. The GFRP confinement enhancement in Pier 2 and Pier 3 is not sufficiently adequate to avoid crushing of the concrete elements under additional forces. This force redistribution can be seen in the marginal improvement in strength in the last two cycles of the analysis. Therefore, it is crucial to consider the influence of the component-level response on the system-level behaviour in order to provide the most effective repair strategy.

6. Conclusions

The following conclusions can be drawn from the conducted studies:

1. Unlike commonly used methods which are based on oversimplified formulations or limited to component-level analysis of repaired structures, the proposed multi-scale procedure enables analysis of entire structural system while considering the local behaviour of repaired components in a computationally and memory efficient manner.
2. For axially loaded members such as bridge piers and columns, the buckling of longitudinal reinforcement and damage effects prior to repair can significantly affect the response of the repaired structure. The influence of these mechanisms were investigated in the application example section.
3. The analysis procedure was able to successfully capture the peak load, ductility and energy dissipation of RC columns confined with GFRP layers.
4. There was a tendency to overestimate the peak loads for specimens with more than two layers of GFRP sheets. This may be a consequence of slip between layers of FRP sheets or lower effective confinement due to the square shape of the columns, known as arching action.
5. For RC columns without GFRP layers, the analysis predicted cover spalling followed by yielding of the transverse reinforcement and buckling of the longitudinal bars as the failure mode; for specimens with GFRP layers, confinement effects prevented the concrete spalling and the failure occurred as a result of rupture of the GFRP sheets. The computed failure modes agreed well with the experimentally observed behaviour.
6. The RC bridge example demonstrated the importance of considering the influence of component-level analysis on the system-level behaviour and realizing the force redistribution effects on the structure in order to have an effective and efficient repair strategy.

7. Acknowledgments

Financial support provided by IC-IMPACTS (the India-Canada Centre for Innovative Multidisciplinary Partnerships to Accelerate Community Transformation and Sustainability) are gratefully acknowledged.

8. References

[1] Lam L, Teng J (2002): Strength models for fiber-reinforced plastic-confined concrete. *J. Struct. Eng., ASCE,* **128** (5), 612-623.

[2] Karbhari VM, Gao Y (1997): Composite jacketed concrete under uniaxial compression-verification of simple design equations. *J. Mater. Civ. Eng., ASCE,* **9** (4), 185-193.

[3] Saafi M, Toutanji HA, Li Z (1999): Behavior of concrete columns confined with fiber reinforced polymer tubes. *ACI Mater. J.,* **96** (4), 500-509.

[4] Memon MS, Sheikh S (2005): Seismic resistance of square concrete columns retrofitted with glass fiber-reinforced polymer. *ACI Struct. J.,* **102** (5), 774-783.

[5] Zhu Z, Ahmad I, Mirmirana A (2006): Fiber element modeling for seismic performance of bridge columns made of concrete-filled FRP tubes. *Eng. Struct.*, **28** (14), 2023-2035.

[6] OpenSees [Computer software]: Pacific Earthquake Engineering Research Center, Univ. of California, Berkeley.

[7] Samaan M, Mirmiran A, Shahawy M (1998): Model of concrete confined by fiber composite. *J. Struct. Eng., ASCE*, **124** (9), 1025-31.

[8] Taucer FF, Spacone E, Filippou FC (1991): A fiber beam-column element for seismic response analysis of RC structures. *Technical Report*, Earthquake Engineering Research Center, University of California, Berkeley

[9] Teng J, Lam L, Lin G, Lu J, Xiao Q (2016): Numerical simulation of FRP-jacketed RC columns subjected to cyclic and seismic loading. *J. Compos. Constr., ASCE*, **20** (1).

[10] Lam L, Teng J (2009): Stress-Strain model for FRP confined concrete under cyclic axial compression. *Eng. Struct., ASCE*, **1** (2), 308–321.

[11] Rougier VC, Luccioni BM (2007): Numerical assessment of FRP retrofitting systems for reinforced concrete elements. *Eng. Struct.* **29** (8), 1664-1675.

[12] Karabinis AI, Rousakis TC, Manolitsi GE (2008): 3D finite-element analysis of substandard RC columns strengthened by fiber-reinforced polymer sheets. *J. Compos. Constr., ASCE*, **12** (5), 531-540.

[13] ABAQUS [Computer Software]: Hibbit, Karlsson and Sorensen Inc., ABAQUS/PRE users' manual.

[14] Yalcin C, Saatcioglou M (2000): Inelastic analysis of RC columns. *Comput. Struct.*,**77** (5), 539-555.

[15] Montoya E, Vecchio FJ, Sheikh SA (2004): Numerical evaluation of the behaviour of steel- and FRP-confined concrete columns using compression field modelling. *Eng Struct*, **26** (11), 1535-1545.

[16] Eslami A, Ronagh HR (2013): Effect of FRP wrapping in seismic performance of RC buildings with and without special detailing – A case study. *Compos. Part B: Eng. J.*, **45** (1), 1265-1274.

[17] Galal K, El-Sokkary H (2008): Analytical evaluation of seismic performance of RC frames rehabilitated using FRP for increased ductility of members. *J. Perform. Constr. Fac., ASCE*, **22** (5), 276-288.

[18] Garcia R, Hajirasouliha I, Pilakoutas K (2010): Seismic behaviour of deficient RC frames strengthened with CFRP composites. *Eng. Struct. J.*, **32** (10), 3075-3085.

[19] Vecchio FJ (2000): Disturbed stress field model for reinforced concrete: Formulation. *J. Struct. Eng., ASCE*, **126** (8), 1070-1077.

[20] Sadeghian V, Vecchio FJ, Kwon O (2015): An integrated framework for analysis of mixed-type reinforced concrete structures. CompDyn 2015, Crete, Greece.

[21] Guner S, Vecchio FJ (2011): Analysis of shear-critical reinforced concrete plane frame elements under cyclic loading. *J. Struct. Eng., ASCE*, **137** (8), 834-843.

[22] Sadeghian V, Vecchio FJ (2014): Cyrus user's manual. University of Toronto, Toronto, Canada.

[23] Wong PS, Vecchio FJ, Trommels H (2013): VecTor2 user's manual. University of Toronto, Toronto, Canada.

[24] Vecchio FJ (1999): Towards cyclic load modelling of reinforced concrete. *ACI Struct. J.*, **96** (2), 193-202.

[25] Seckin M (1981): Hysteretic behaviour of cast-in-place exterior beam-column-slab subassemblies. Department of Civil Engineering, University of Toronto, Ph.D.

[26] Dhakal RP, Maekawa K (2002): Modeling for post-yield buckling of reinforcement. *J. Struct. Eng., ASCE*, **128** (9), 1139-1147.

[27] Nakaba K, Kanakubo T, Furuta T, Yoshizawa H (2001): Bond behavior between fiber-reinforced polymer laminates and concrete. *ACI Struct. J.*, **98** (3) 359-367.

[28] Wong R, Vecchio FJ (2003): Towards modeling of reinforced concrete members with externally bonded fiber-reinforced polymer composites. *ACI Struct. J.*, **100** (1), 47-55.

[29] Sato Y, Vecchio FJ (2003): Tension stiffening and crack formation in reinforced concrete members with fiber-reinforced polymer sheets. *J. Struct. Eng., ASCE*, **129** (6), 717-724.

[30] Sadeghian V, Vecchio FJ, Kwon O (under review): Analysis of large shear-critical reinforced concrete structures repaired with fibre-reinforced polymer sheets. *Durability of Repairs Special Issue, Innovations in Corrosion and Materials Science Journal.*